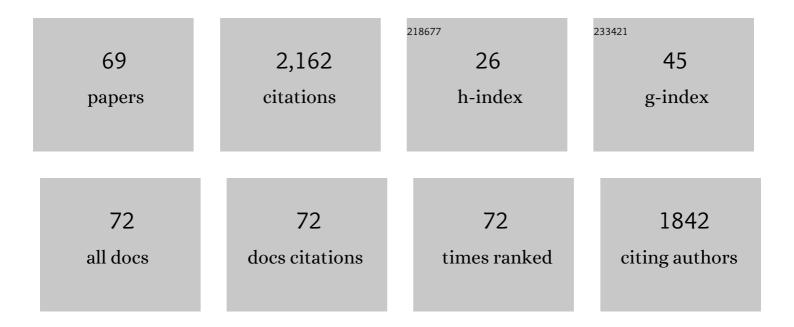
List of Publications by Year in descending order

Source: https://exaly.com/author-pdf/6288984/publications.pdf Version: 2024-02-01



#	Article	IF	CITATIONS
1	Use of Nonâ€Matrix Matched Reference Materials for the Accurate Analysis of Calcium Carbonate by LAâ€ICPâ€MS. Geostandards and Geoanalytical Research, 2022, 46, 97-115.	3.1	5
2	Novel Methods to Manipulate Autolysis in Sparkling Wine: Effects on Yeast. Molecules, 2021, 26, 387.	3.8	9
3	Assessment of the mineral ilmenite for U–Pb dating by LA-ICP-MS. Journal of Analytical Atomic Spectrometry, 2021, 36, 1244-1260.	3.0	9
4	Quantitative WDS compositional mapping using the electron microprobe. American Mineralogist, 2021, 106, 1717-1735.	1.9	17
5	Phase relations of arsenian pyrite and arsenopyrite. Ore Geology Reviews, 2021, 136, 104285.	2.7	9
6	Dissolution of mantle orthopyroxene in kimberlitic melts: Petrographic, geochemical and melt inclusion constraints from an orthopyroxenite xenolith from the Udachnaya-East kimberlite (Siberian) Tj ETQq0	001g8T/(Dve t lock 10 T
7	A genetic story of olivine crystallisation in the Mark kimberlite (Canada) revealed by zoning and melt inclusions. Lithos, 2020, 358-359, 105405.	1.4	7
8	Evolution of kimberlite magmas in the crust: A case study of groundmass and mineral-hosted inclusions in the Mark kimberlite (Lac de Gras, Canada). Lithos, 2020, 372-373, 105690.	1.4	11
9	Carbonates at the supergiant Olympic Dam Cu-U-Au-Ag deposit, South Australia. Part 1: Distribution, textures, associations and stable isotope (C, O) signatures. Ore Geology Reviews, 2020, 126, 103775.	2.7	4
10	Polymineralic inclusions in oxide minerals of the Afrikanda alkaline-ultramafic complex: Implications for the evolution of perovskite mineralisation. Contributions To Mineralogy and Petrology, 2020, 175, 1.	3.1	6
11	Kimberlite genesis from a common carbonate-rich primary melt modified by lithospheric mantle assimilation. Science Advances, 2020, 6, eaaz0424.	10.3	72
12	High Lability Fe Particles Sourced From Glacial Erosion Can Meet Previously Unaccounted Biological Demand: Heard Island, Southern Ocean. Frontiers in Marine Science, 2019, 6, .	2.5	25
13	New Olivine Reference Material for <i>In Situ</i> Microanalysis. Geostandards and Geoanalytical Research, 2019, 43, 453-473.	3.1	77
14	Polymineralic inclusions in kimberlite-hosted megacrysts: Implications for kimberlite melt evolution. Lithos, 2019, 336-337, 310-325.	1.4	25
15	Multipoint Background Analysis: Gaining Precision and Accuracy in Microprobe Trace Element Analysis. Microscopy and Microanalysis, 2019, 25, 30-46.	0.4	22
16	Djerfisherite in kimberlites and their xenoliths: implications for kimberlite melt evolution. Contributions To Mineralogy and Petrology, 2019, 174, 1.	3.1	16
17	Composition and emplacement of the Benfontein kimberlite sill complex (Kimberley, South Africa): Textural, petrographic and melt inclusion constraints. Lithos, 2019, 324-325, 297-314.	1.4	43
18	Diversity in Ruby Geochemistry and Its Inclusions: Intra- and Inter- Continental Comparisons from Myanmar and Eastern Australia. Minerals (Basel, Switzerland), 2019, 9, 28.	2.0	18

#	Article	IF	CITATIONS
19	Geochemistry and provenance of the Turquoise Bluff Slate, northeastern Tasmania: tectonic significance. Australian Journal of Earth Sciences, 2019, 66, 227-246.	1.0	3
20	The Dovyren Intrusive Complex (Southern Siberia, Russia): Insights into dynamics of an open magma chamber with implications for parental magma origin, composition, and Cu-Ni-PGE fertility. Lithos, 2018, 302-303, 242-262.	1.4	28
21	Significance of halogens (F, Cl) in kimberlite melts: Insights from mineralogy and melt inclusions in the Roger pipe (Ekati, Canada). Chemical Geology, 2018, 478, 148-163.	3.3	19
22	Monticellite in group-I kimberlites: Implications for evolution of parental melts and post-emplacement CO2 degassing. Chemical Geology, 2018, 478, 76-88.	3.3	35
23	Ultrastructural Integrity of Human Capsulotomies Created by a Thermal Device. Ophthalmology, 2018, 125, 340-344.	5.2	10
24	Comparison and Combination of Energy and Wavelength Dispersive X-Ray Spectrometry in Electron Probe Microanalysis of Minerals and Glasses. Microscopy and Microanalysis, 2018, 24, 748-749.	0.4	3
25	Textural evolution of perovskite in the Afrikanda alkaline–ultramafic complex, Kola Peninsula, Russia. Contributions To Mineralogy and Petrology, 2018, 173, 1.	3.1	10
26	Reply. Ophthalmology, 2018, 125, e73-e74.	5.2	0
27	Intraoperative performance and ultrastructural integrity of human capsulotomies created by the improved precision pulse capsulotomy device. Journal of Cataract and Refractive Surgery, 2018, 44, 1333-1335.	1.5	10
28	Origin of complex zoning in olivine from diverse, diamondiferous kimberlites and tectonic settings: Ekati (Canada), Alto Paranaiba (Brazil) and Kaalvallei (South Africa). Mineralogy and Petrology, 2018, 112, 539-554.	1.1	43
29	Was Crustal Contamination Involved in the Formation of the Serpentine-Free Udachnaya-East Kimberlite? New Insights into Parental Melts, Liquidus Assemblage and Effects of Alteration. Journal of Petrology, 2018, 59, 1467-1492.	2.8	38
30	Applications of hyperspectral mineralogy for geoenvironmental characterisation. Minerals Engineering, 2017, 107, 63-77.	4.3	34
31	The final stages of kimberlite petrogenesis: Petrography, mineral chemistry, melt inclusions and Sr-C-O isotope geochemistry of the Bultfontein kimberlite (Kimberley, South Africa). Chemical Geology, 2017, 455, 342-356.	3.3	78
32	Different types of liquid immiscibility in carbonatite magmas: A case study of the Oldoinyo Lengai 1993 lava and melt inclusions. Chemical Geology, 2017, 455, 376-384.	3.3	22
33	Prediction of Mineral Dust Properties at Mine Sites. , 2017, , 343-354.		0
34	Cu–Ni–PGE fertility of the Yoko-Dovyren layered massif (northern Transbaikalia, Russia): thermodynamic modeling of sulfide compositions in low mineralized dunite based on quantitative sulfide mineralogy. Mineralium Deposita, 2016, 51, 993-1011.	4.1	29
35	Matrix effects in Pb/U measurements during LA-ICP-MS analysis of the mineral apatite. Journal of Analytical Atomic Spectrometry, 2016, 31, 1206-1215.	3.0	71
36	A story of olivine from the McIvor Hill complex (Tasmania, Australia): Clues to the origin of the Avebury metasomatic Ni sulfide deposit. American Mineralogist, 2016, 101, 1321-1331.	1.9	14

#	Article	IF	CITATIONS
37	U–Th–Pb monazite dating and the timing of arc–continent collision in East Timor. Australian Journal of Earth Sciences, 2016, 63, 367-377.	1.0	7
38	Postmagmatic magnetite–apatite assemblage in mafic intrusions: a case study of dolerite at Olympic Dam, South Australia. Contributions To Mineralogy and Petrology, 2016, 171, 1.	3.1	15
39	Improved methodology for the microwave digestion of carbonate-rich environmental samples. International Journal of Environmental Analytical Chemistry, 2016, 96, 119-136.	3.3	17
40	Constraints on kimberlite ascent mechanisms revealed by phlogopite compositions in kimberlites and mantle xenoliths. Lithos, 2016, 240-243, 189-201.	1.4	111
41	Precious metals in gossanous waste rocks from the Iberian Pyrite Belt. Minerals Engineering, 2016, 87, 45-53.	4.3	11
42	Gold and Arsenopyrite Exsolution and Limits of Arsenic Solubility in Pyrite Investigated by SEM, EPMA, and L-ICPMS. Microscopy and Microanalysis, 2015, 21, 1229-1230.	0.4	0
43	The evolution of authigenic Zn–Pb–Fe-bearing phases in the Grieves Siding peat, western Tasmania. Contributions To Mineralogy and Petrology, 2015, 170, 1.	3.1	10
44	Chemical abrasion of zircon and ilmenite megacrysts in the Monastery kimberlite: Implications for the composition of kimberlite melts. Chemical Geology, 2014, 383, 76-85.	3.3	42
45	Petrogenesis of Mantle Polymict Breccias: Insights into Mantle Processes Coeval with Kimberlite Magmatism. Journal of Petrology, 2014, 55, 831-858.	2.8	86
46	Fractionation of sulphur relative to iron during laser ablation-ICP-MS analyses of sulphide minerals: implications for quantification. Journal of Analytical Atomic Spectrometry, 2014, 29, 1024-1033.	3.0	46
47	Anterior Capsulotomy Integrity after Femtosecond Laser-Assisted Cataract Surgery. Ophthalmology, 2014, 121, 17-24.	5.2	142
48	Authigenic monazite and detrital zircon dating from the Proterozoic Rocky Cape Group, Tasmania: Links to the Belt-Purcell Supergroup, North America. Precambrian Research, 2014, 250, 50-67.	2.7	77
49	Determination of Trace Elements in Quartz by Combined EPMA and CL Microspectrometry. Microscopy and Microanalysis, 2014, 20, 718-719.	0.4	2
50	Diversity of primary CL textures in quartz from porphyry environments: implication for origin of quartz eyes. Contributions To Mineralogy and Petrology, 2013, 166, 1253-1268.	3.1	20
51	Parental carbonatitic melt of the Koala kimberlite (Canada): Constraints from melt inclusions in olivine and Cr-spinel, and groundmass carbonate. Chemical Geology, 2013, 353, 96-111.	3.3	72
52	Evidence for an Intrabasinal Source and Multiple Concentration Processes in the Formation of the Carbon Leader Reef, Witwatersrand Supergroup, South Africa. Economic Geology, 2013, 108, 1215-1241.	3.8	63
53	Cathodoluminescence properties of quartz eyes from porphyry-type deposits: Implications for the origin of quartz. American Mineralogist, 2013, 98, 98-109.	1.9	31
54	Nickel-rich metasomatism of the lithospheric mantle by pre-kimberlitic alkali-S–Cl-rich C–O–H fluids. Contributions To Mineralogy and Petrology, 2013, 165, 155-171.	3.1	26

4

#	Article	IF	CITATIONS
55	Mineralogy and Formation of Black Smoker Chimneys from Brothers Submarine Volcano, Kermadec Arc. Economic Geology, 2012, 107, 1613-1633.	3.8	107
56	Nature of alkali-carbonate fluids in the sub-continental lithospheric mantle. Geology, 2012, 40, 967-970.	4.4	88
57	Challenges in Electron Probe Micronalysis 60 Years after Castaing: Examples from Complex Uranium and Rare Earth Element Minerals from Northern Australian Ore Deposits. Microscopy and Microanalysis, 2011, 17, 578-579.	0.4	1
58	An Investigation into the General Applicability of Quantification of Trace Ti in Quartz by Cathodoluminescence. Microscopy and Microanalysis, 2010, 16, 808-809.	0.4	2
59	Electronic structure and topography of annealed SrTiO3(111) surfaces studied with MIES and STM. Applied Surface Science, 2005, 252, 196-199.	6.1	7
60	Sr diffusion in undoped and La-doped SrTiO3single crystals under oxidizing conditions. Physical Chemistry Chemical Physics, 2005, 7, 2053-2060.	2.8	122
61	Changes in the surface topography and electronic structure of SrTiO3(110) single crystals heated under oxidizing and reducing conditions. Surface Science, 2004, 566-568, 105-110.	1.9	20
62	Ti diffusion in La-doped SrTiO3single crystals. Physical Chemistry Chemical Physics, 2004, 6, 3639-3644.	2.8	58
63	MACROCRYSTALS OF Pt Fe ALLOY FROM THE KONDYOR PGE PLACER DEPOSIT, KHABAROVSKIY KRAY, RUSSIA: TRACE-ELEMENT CONTENT, MINERAL INCLUSIONS AND REACTION ASSEMBLAGES. Canadian Mineralogist, 2004, 42, 601-617.	1.0	41
64	Nanostructures on La-doped SrTiO3 surfaces. Analytical and Bioanalytical Chemistry, 2003, 375, 924-928.	3.7	10
65	Island formation on 0.1 at.% La-doped SrTiO3(100) at elevated temperatures under reducing conditions. Surface Science, 2003, 523, 80-88.	1.9	35
66	Study of the electronic and atomic structure of thermally treated SrTiO3(110) surfaces. Surface and Interface Analysis, 2003, 35, 998-1003.	1.8	23
67	Cation Transport and Surface Reconstruction in Lanthanum Doped Strontium Titanate at High Temperatures. Materials Research Society Symposia Proceedings, 2002, 756, 1.	0.1	1
68	Geometric structure and chemical composition of SrTiO3 surfaces heated under oxidizing and reducing conditions. Surface Science, 2002, 507-510, 447-452.	1.9	23
69	Title is missing!. , 2002, 8, 221-228.		19